Available online at www.sciencedirect.com
ScienceDirect
Tetrahedron
Tetrahedron 63 (2007) 7375–7385

Molecular organogels of the sodium salt of (*R*)-12-hydroxystearic acid and their templated syntheses of inorganic oxides

Xiao Huang and Richard G. Weiss*

Department of Chemistry, Georgetown University, 37th and O Streets, NW, Washington, DC 20057-1227, USA

Received 12 October 2006; revised 8 December 2006; accepted 1 February 2007
Available online 7 February 2007

Abstract—(*R*)-12-Hydroxystearic acid (HSA), a natural product from castor oil, is a well-known low-molecular mass organogelator (LMOG). Here, we demonstrate that the sodium salt of HSA, HSA-S, is an extremely versatile and efficient LMOG. Furthermore, its self-assembled fibrillar networks (SAFINs) in gels with ethanol, benzene, tetrahydrofuran, and dimethyl sulfoxide, as well as the gel of HSA with benzene, are shown to act as templates during the sol–gel polymerization of tetraethyl orthosilicate (TEOS) in the absence or presence of an external catalyst. The templated, fiber-like objects obtained after calcinations have been characterized. The shape of the templated silica is strongly influenced by the catalyst applied. In addition, it has been possible to effect the formation of assemblies of nanoscale objects of Fe_2O_3 and CuO by polymerization of appropriate precursors in HSA-S based gels and in suspensions, respectively, followed by drying and calcination. The procedures employed are efficient and inexpensive protocols to make porous nanomaterials using organogels. Typically, templated syntheses of such materials in organogels have employed less accessible and more structurally complex LMOGs than HSA-S or HSA. Electrostatic interactions via Na^+ bridges or H-bonding between silicate intermediates and gelator strands are proposed to be a primary driving force for templating.

1. Introduction

During the past several years, a great deal of attention has been focused on the syntheses of nanostructured materials with different shapes and structures due to their potential applications as catalysts and matrices for separations and as building blocks for nanodevices.[1] One effective and simple method to make such materials is templated syntheses in which the templates consist of self-assembled organic molecules because the templates are easily removed after the materials have been formed.[2] Molecular organogels, which consist usually of <2 wt % of a low-molecular mass organic gelator (LMOG) and a liquid,[3] are also potentially attractive templates[4–6] due to the 10–100 nm (monodisperse in many cases) cross-sections of the fibers, which constitute their self-assembled fibrillar networks (SAFINs).[3] To date, the structures of the LMOGs in organogels used for templated formation of materials have been somewhat complex molecules, which are available only through sometimes laborious synthetic procedures.[4–6] In an attempt to develop molecular organogels with simpler and more easily accessible LMOGs, we have investigated in detail the templating properties of a series of tetraalkylphosphonium salts.[7] These salts are prepared in good yields from the corresponding tri-alkylphosphines in one or two simple steps. Here, we report our observations with the naturally occurring and commercially available LMOG, (*R*)-12-hydroxystearic acid (HSA, a major component of castor oil[8]), and HSA-S, the sodium salt of HSA. HSA is a known LMOG of a limited number of liquids,[9] and gels of some of its salts have been studied extensively.[10] We find that HSA-S is an exceedingly efficient LMOG for a much wider range of organic liquids than the parent acid[11] and that the SAFINs of its gels as well as those of HSA can act as templates for the shape-directed syntheses of silica from tetraethyl orthosilicate (TEOS) and of other inorganic oxides. The materials made in this way are very porous and most have high aspect ratios. Our results indicate that the location where the sol–gel process is initiated in the organogel has a strong influence on the silica morph obtained.[7] Thus, it is exceedingly important to devise systems for templating in which the surfaces of the templates and the intermediates leading to the material of interest be attracted to each other.

The mechanism of the hydrolytic sol–gel process of tetraalkyl orthosilicates has been studied extensively.[12] It occurs via anionic intermediates when the pH is above the isoelectric point of the silica precursor, ~2 for TEOS,[12] and cationic when the pH is below the isoelectric point.[12] It has been demonstrated mainly by Shinkai[4] and recently

Keywords: Organogel; (*R*)-12-Hydroxystearic acid; Sol–gel process; Silica; Template synthesis.
* Corresponding author. Tel.: +1 202 687 6013; fax: +1 202 687 6209; e-mail: weissr@georgetown.edu

0040–4020/$ - see front matter © 2007 Published by Elsevier Ltd.
doi:10.1016/j.tet.2007.02.008

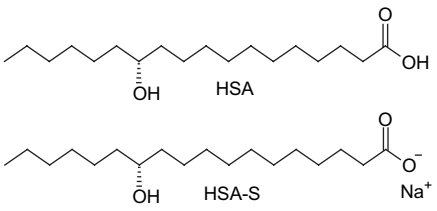

Chart 1. Structures of LMOGs employed.

by us[7] that strong interactions between anionic silicate intermediates and gelator templates (and, thus, polymerization occurring mainly on the surface of the templates) are the key to templated syntheses. As a result, most LMOGs, which have been successful in making templated porous silica and other inorganic polymeric materials are either cationic or neutral and have amine functional groups.[4–6]

12-Hydroxystearic acid and especially its calcium and lithium salts have been studied extensively because of their utilization as greases and plastic lubricants.[13] Gels of HSA,[9] as well as the helical fibers of its SAFINS with some liquids,[10] are also well-documented. Except for the pioneering studies by McClellan[10a] and Tachibana and Kambara,[10b–d] molecular gels employing HSA salts appear to have been ignored and there is only one report of gels with HSA-S as the LMOG, which we have been able to find.[11] For that reason, we have emphasized results with HSA-S here.

HSA and its sodium salt are a relatively strong acid and base, respectively, which can catalyze sol–gel processes in the absence of external catalysts. Thus, when these LMOGs are aggregated in SAFINs of molecular gels, initiation of a sol–gel process is more prone to occur at the surfaces of the constituent fibers than in the liquid bulk and templated materials are expected. In HSA-based molecular gels, the anionic silicate intermediates (at pH >2) are attracted to the template surface by H-bonding interactions. Interactions in which Na^+ ions act as electrostatically attractive 'bridges'[2c,g] between fibers of HSA-S LMOGs and anionic silicates appear to be responsible for the templated materials in those gels; the paucity of examples of assemblies of carboxylate gelators as successful templates[7] may be due to the expectation that electrostatic repulsion between the surface negative charges on the SAFINs and the negatively charged silicate intermediates will inhibit the 'bridging' interactions (Chart 1).

2. Results and discussions

2.1. Gelation studies

The gelation of racemic and chiral HSA molecules has been studied extensively.[9] HSA can gelate several hydrocarbon and chlorinated liquids, and many of these gels are transparent.[9] Although the lithium, calcium, and aluminum salts of HSA, especially, are known to form helical aggregates,[10] which thicken various liquids,[13] the gelation ability of HSA salts has not been well explored.[10] Table 1 summarizes the gelation tests of HSA-S and shows that it is a much more versatile gelator than HSA. Like those of HSA, many of the gels containing only 0.5 wt % HSA-S are transparent or translucent. In fact, HSA-S is relatively insoluble in many of the liquids examined in Table 1 and could not be dissolved in them at 1 wt %. For that reason, it was necessary to boil some of the liquids and to add 10 wt % methanol to them to dissolve even 0.5 wt % of the salt.

Table 1. Gelation tests with 0.5 wt % HSA-S and 1.0 wt % HSA as LMOGs and various organic liquids and water[a]

Solvent	HSA-S	T_{gel} (°C)	Period of stability	HSA
n-Dodecane	CG+liquid			
n-Dodecane[b]	TG	60.0–60.5	~2 weeks	TG[9a,b]
Benzene	ppt			CG[9a,b]
THF	TG	73.0–78.5	>6 months	Sol
THF[b]	TG	>100	>6 months	Sol
Acetone[c]	TG	46.5–71.5	~1 day	Sol
Acetonitrile[c]	TG	49.5–65.5	~1 day	ppt
Ethyl acetate[c]	OG	50.0–72.0	~2 days	Sol
Chloroform[c]	CG	47.0–61.5	~1 day	CG[9d,e]
Carbon tetrachloride	CG	50.0–62.5	~2 days	CG[9d,e]
DMF	CG	91.5–98.5	>6 months	Sol
DMF[b]	TG	>100	>6 months	Sol
DMSO	CG	53.0–65.5	>6 months	Sol
DMSO[b]	TG	>100	>6 months	Sol
Methanol	Sol			Sol
Ethanol	ppt (slowly)			Sol
Ethanol[b]	OG	61.0–84.5	~3 months	Sol
Water	Thick suspension			ppt

[a] CG: clear gel; TG: translucent gel; OG: opaque gel; ppt: precipitate; sol: solution.
[b] HSA-S of 4 wt %.
[c] Methanol (10 wt %) added to improve solubility; the mixture in the flame-sealed container was heated to boiling for several minutes to attain a solution/sol.[14]

Dimethyl sulfoxide (DMSO), tetrahydrofuran (THF), and dimethylformamide (DMF) were the exceptions—their gels at 0.5–4.0 wt % of HSA-S, possessing excellent thermal and temporal stabilities, could be prepared with these liquids without the addition of methanol. In that regard, note that the temperatures at which the gel phases of some of the gel phases in Table 1 were converted to sols or were destroyed, T_{gel}, are higher than the boiling temperatures of the liquid components!

Most of the gels in Table 1 are transparent or nearly transparent in that no discernible birefringence was observed by polarized optical microscopy and the very low concentration of HSA-S precluded the observation of diffraction of X-rays from their SAFINs. However, the gels with 4 wt % HSA-S in *n*-dodecane, ethanol, DMF, THF, and DMSO could be examined by X-ray diffraction and polarized optical microscopy. The optical micrograph in Figure 1a indicates that the 4 wt % HSA-S/ethanol gel is a microphase-separated system. The absence of clear features attributable to the SAFINs in Figure 1c and e indicates that the component fibers in THF (DMSO and DMF gels provide similar micrographs) and *n*-dodecane gels are much smaller than those in the ethanol gel. Figure 1b and d shows the powder X-ray diffraction patterns of 4 wt % HSA-S organogels in ethanol, THF, DMSO, and DMF. The diffractograms demonstrate that the packing arrangements for the SAFINs in these gels are lamellar and are very similar to that found for neat HSA-S (the progression of the *d*-spacing of the low-angle

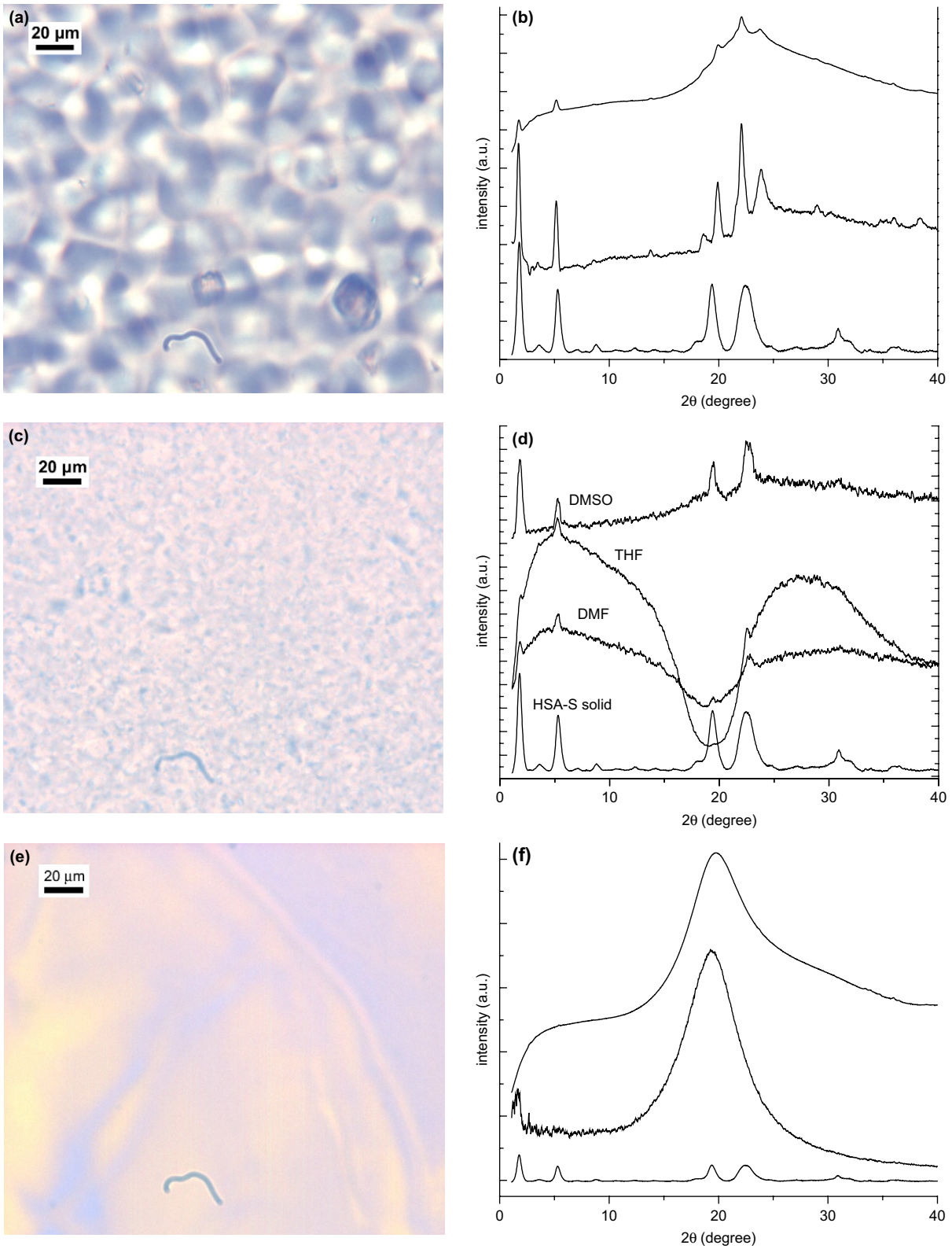

Figure 1. Polarized optical micrographs of 4.0 wt % HSA-S gels in ethanol (a), THF (c), and *n*-dodecane (e). Powder X-ray diffraction patterns of (b) 4.0 wt % ethanol gel (top), solvent background deducted empirically from ethanol gel diffraction (middle), and neat HSA-S crystal (bottom); (d) 4.0 wt % DMSO, THF, and DMF gels after empirical subtraction of solvent components and neat HSA-S crystal; (f) *n*-dodecane gel (top) and after empirical subtraction of solvent component (middle) and neat HSA-S crystal (bottom).

peaks from the Bragg relationship is: 1:1/2:1/3:1/4:1/5[15]). Since the *d*-spacing corresponding to the lowest angle peak is ca. 49.5 Å, the lamellae units must be bilayers (see Fig .1).

However, almost no discernible diffraction could be observed from the 4 wt % HSA-S/*n*-dodecane gel. Its transparent appearance and lack of a Tyndall effect indicate that the cross-sections of the primary objects responsible for its

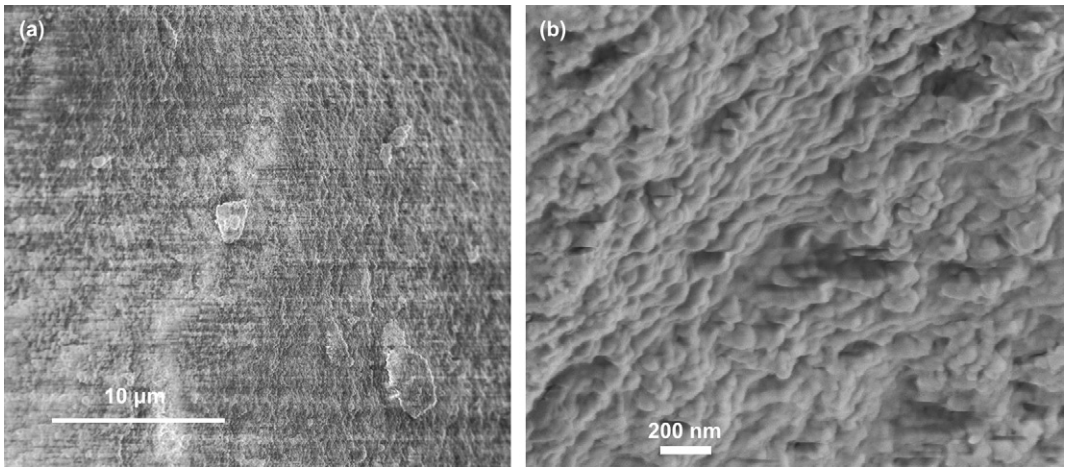

Figure 2. SEM images at different magnifications of silica isolated from gels containing 4 wt % HSA and 90:10 (w/w) benzene/TEOS without external catalyst.

SAFIN may be too small to allow effective correlation lengths for diffraction of the X-rays. After empirical subtraction of scattering from the solvent background, a small peak at ca. 1.8°, as found for neat HSA-S, could be detected (Fig. 1f); we therefore believe that the *n*-dodecane gels are also in bilayers as well.

The estimated HSA-S anion chain length is ~23.4 Å[16] and the van der Waals radius of a sodium cation is ca. 1.03 Å.[17] On this basis, the HSA-S chains within the SAFINs must be packed in a non-interdigitated or very slightly interdigitated arrangement and oriented orthogonal to the bilayer planes. In the ethanol gel, the peaks at >15° are in different positions and intensities from those of the neat crystal; this observation requires that the *intralayer* packing arrangement in the SAFINs of this gel be different from that of the DMSO, THF, and DMF gels whose higher angle diffractions match those of neat HSA-S.

2.2. Template synthesis

2.2.1. (*R*)-12-Hydroxystearic acid as template. HSA is a very good gelator of many hydrocarbon and chlorinated liquids.[7,9] A 4 wt % HSA/benzene gel is employed here to investigate the templated synthesis of silica. The silica obtained from it and from HSA-S is amorphous according to powder X-ray diffraction measurements (not shown).

The fiber-like silica objects from the 4 wt % HSA/benzene gel in the absence of an external catalyst are shown in Figure 2a and b. The cross-sections of these objects, tens of nanometers, are much thinner than the fibers obtained from polymerization of TEOS in gels consisting of phosphonium salt LMOGs and benzene liquid.[7] This is probably because the cross-sections of the fibers in SAFINs of the transparent HSA/benzene gels are much narrower than those of the opaque phosphonium salt/benzene gels.

Since HSA is the only catalyst present in its benzene gels, H-bonding between the carboxylic acid groups and silicate intermediates is the probable cause of the successful silica templating. If the silicates are held near the surfaces of the SAFIN fibers as they grow, the eventually formed silica should retain some of the shape characteristics of the gel fibers. Although Figure 2b shows that the silica fibers possess some curved features, it was not possible to discern whether they replicate the chirality of the HSA assemblies[9a] or are due to the hydrophobic nature of the benzene liquid[7] and differential surface energies of the silica with the liquid.[18]

Attempts to determine the effect of another acid catalyst, acetic acid, were not successful. When 3 wt % acetic acid was added to the hot 4 wt % HSA/benzene sol, the mixture precipitated upon cooling to room temperature (22 °C). It is reasonable to assume that the acetic acid interrupted the dimeric interactions of HSA molecules, which lead to bilayer (and, therefore, to fiber and SAFIN) formation.

2.2.2. (*R*)-12-Hydroxystearic acid sodium salt as template. Based on the results in Table 1, gels with HSA-S and either ethanol (a protic liquid), THF, or DMSO (two aprotic liquids) were chosen for study as potential templates for TEOS sol–gel polymerization.

Short, rod-like silica objects a few microns in length, which are strings or bundles of spherical particles with diameters ~200 nm, were obtained after calcination of gels consisting of 4 wt % HSA-S and 90:10 (w/w) ethanol/TEOS in the absence of added catalyst (Fig. 3a and b). A small portion of straight and flat rods, a few hundreds of microns in length, was also formed (Fig. 3c). Although the origin of these flat rods is not clear, we suspect that their formation involves H-bonding between the silicate intermediates and ethanol molecules, which is able to weaken the interactions between the silicates and the SAFIN.

Fiber-like silica objects templated from SAFINs of 1 wt % HSA-S and 90:10 THF/TEOS are shown in Figure 4. In the absence of added catalyst, two shapes of silica objects were detected. One resembles the silica particles from gels of 4 wt % HSA and 90:10 (w/w) benzene/TEOS, with ~20 nm cross-sections (Fig. 4a–c), and the other has widths of hundreds of nanometers (see arrows in Fig. 4a). Both types have 'necklace' features (i.e., strings of spherical objects).[4e] In the gels with an added catalyst, only one type of fiber-like object, with 'necklace' features, was isolated, but the size of the cross-section is dependent on the catalyst.

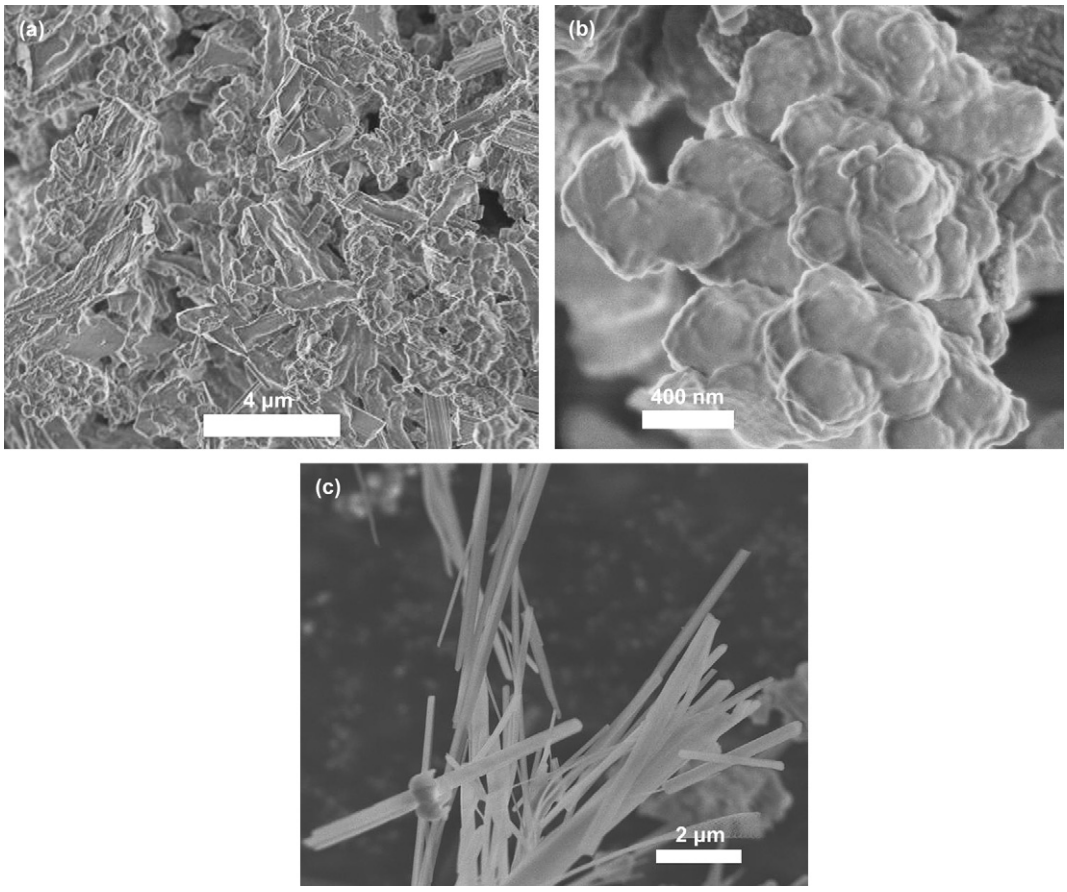

Figure 3. SEM images of silica isolated from gels containing 4 wt % HSA-S and ethanol/TEOS (90:10, w/w) without added catalyst; the gels were aged for one month and calcinated.

We expect that benzyl amine, a neutral molecule with a relatively high pK_b, is a weaker catalyst than concentrated aqueous ammonium hydroxide. With 3 wt % benzyl amine, the fibers have diameters in the range of tens of nanometers (Fig. 4d and e); with 1 wt % of 30% aqueous ammonium hydroxide, the diameters are ~200 nm (Fig. 4f and g).

A possible mechanism to explain these observations is shown in Figure 5. The initiation of the sol–gel process leading to templated material can occur in two principle ways: (1) silicate is generated in the liquid bulk and then is attracted to the template surfaces, the fibers of the SAFINs, by electrostatic forces and (2) silicate is generated initially near the template surface (i.e., surface initiation mechanism[4e]) and remains there. The division among these pathways will depend upon the nature of the liquid, the catalyst, the degree of ion exchange between the surfaces of SAFIN units and the growing silicates (or catalyst), and the LMOG constituting the SAFIN.

The 'necklace' feature observed in many of the silica samples prepared here is a consequence of the deposition or initiation of silicates at a few spots on a template fiber or bundle of fibers rather than evenly along the template.[4e] As the sol–gel process proceeds, silicates grow and join to form 'necklace-like' silica objects. In some cases, the 'necklace' feature is lost as the necklace pieces merge and continue to grow.[7]

In many molecular organogels, the gelator strands are bundles of fibers, as shown in Figure 5. Also, it is known that HSA-S can form chiral aggregates,[10] but we find no evidence that the chirality is transcribed into the templated silica in our cases. When the sol–gel process is initiated in the liquid bulk, the silicates are attracted to the template surfaces of HSA-S fibers by electrostatic interactions. Here, those interactions may take the form of carboxylate–Na^+–silicate bridges when HSA-S is the LMOG[2c] or H-bonding with carboxylic acid groups when HSA is the LMOG. In the bilayer structures of the SAFIN fibers of the HSA and HSA-S molecules, the hydroxyl groups at C12 are buried within the lipophilic octadecyl chains and are H-bonded intermolecularly.[9] As a result, they are not expected to be able to influence the growth of the silicate intermediates. They stabilize the bilayers of the fibers, but do not mediate the location or type of polymerization of TEOS.

Thus, silicates initiated within the bulk and migrating to a fiber bundle are not expected to be able to adopt shapes, which mirror in detail the form of the templates. This will be especially true when the silicate grows to a size comparable to, or larger than, the cross-section of a fiber before it associates with a bundle. Such silicates will be unable to distinguish individual fibers within a bundle. Thus, the final silica objects recovered will reflect the shapes and sizes of bundles of a SAFIN more than its individual fibers. When initial growth of the silicates from TEOS molecules occurs on the surface

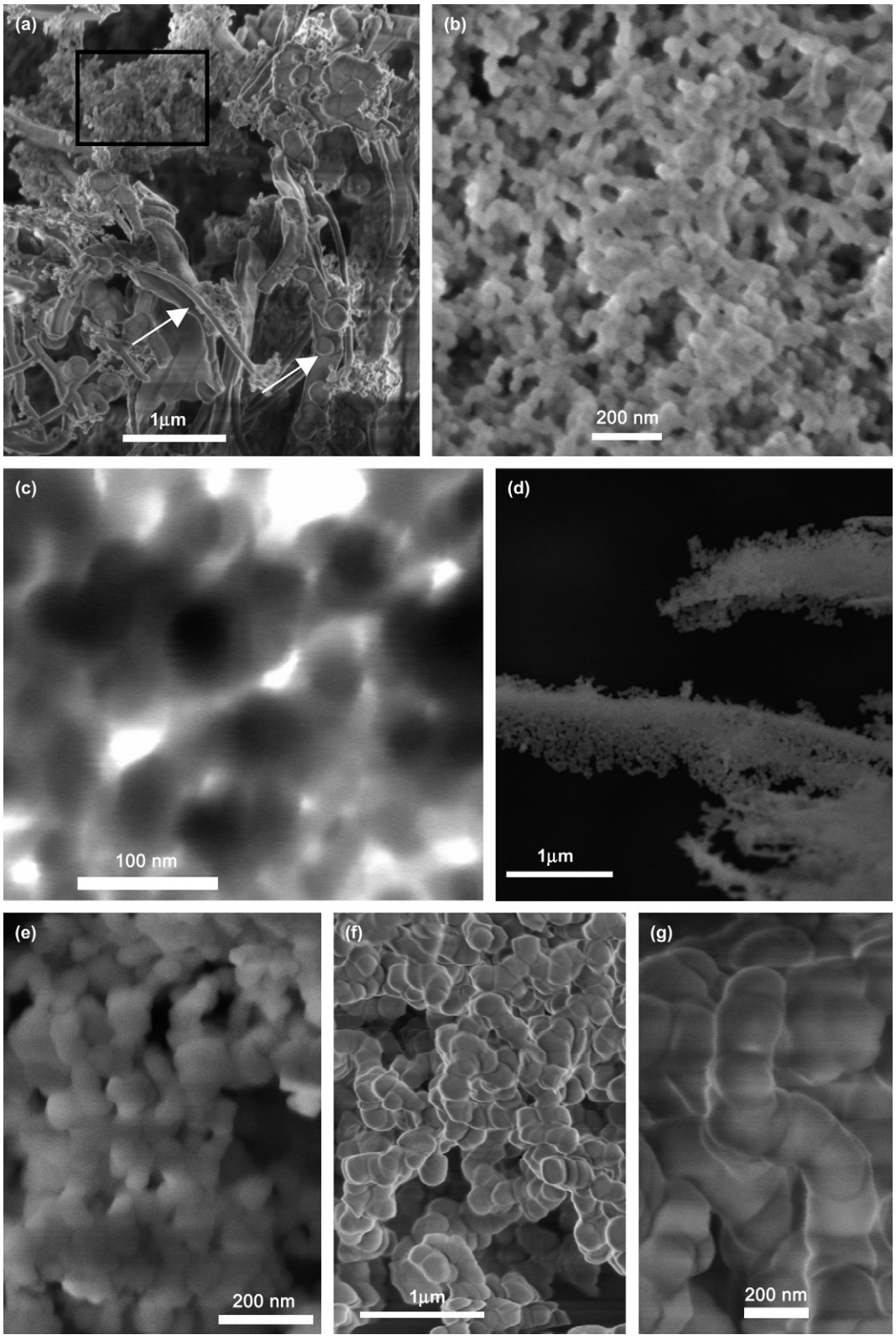

Figure 4. SEM (a,b,d–g) and TEM (c) images of silica isolated from gels of 1 wt % HSA-S and THF/TEOS (90:10, w/w). (a–c) no added catalyst; (b) the square region in (a); (c) TEM of objects in (b); (d,e) ~3 wt % benzyl amine added; (f,g) ~1 wt % 30% aqueous ammonium hydroxide added. All samples were aged for one month and calcinated.

of a fiber, the final silica objects should be able to pattern better the individual fibers and their cross-sections will be narrower than when the silicates are initiated in the liquid bulk.

Both mechanisms appear to be operative in gels of HSA-S with 90:10 THF/TEOS without added catalyst. We conjecture that a small amount of dissolved HSA-S molecules is able to catalyze some of the sol–gel process in the bulk while

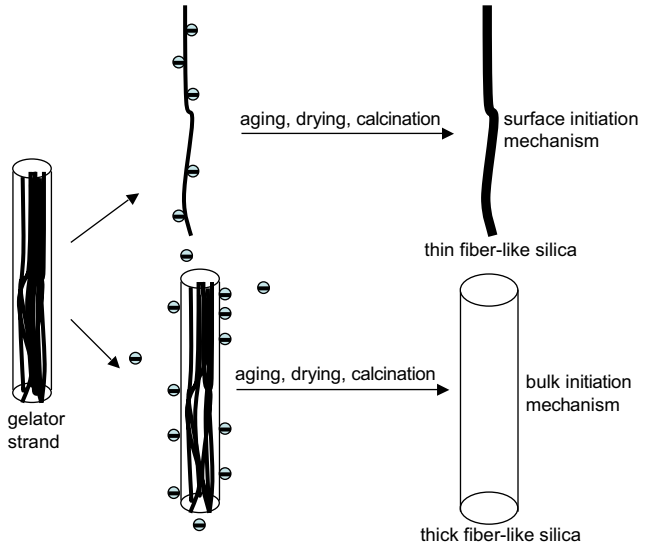

Figure 5. Cartoon representation of templated silica formation via bulk and surface initiation mechanisms. ⊖ represents anionic silicate intermediates.

the majority of the polymerization occurs at SAFIN surfaces. Because HSA-S is much more soluble in ethanol than in THF, most of the silica from HSA-S in 90:10 ethanol/TEOS gel appear to emanate from the liquid bulk; 'necklace' fibers of silica with cross-sections in the hundreds of nanometers are observed.

When a weak catalyst such as benzyl amine is added to HSA-S in 90:10 THF/TEOS gel, 'necklace' silica fibers with cross-sections of only tens of nanometers are obtained. The apparent change to surfaced-dominated initiation is probably due to a combination of factors. The benzyl amine does not promote rapid initiation of silicate intermediates in the bulk and may decrease the concentration of dissolved HSA-S molecules as a result of polarity effects. However, when a stronger catalyst, ammonium hydroxide, is added to the same gel, the bulk initiation mechanism can again dominate, as indicated by the large cross-sections of the 'necklace' silica fibers, ca. 200 nm.

The lack of templated silica objects from gels of HSA-S in 90:10 DMSO/TEOS after drying and calcination is ascribed to the very large surface tension of the liquid.[19] We suspect that templated objects are formed but they collapse during the drying process.[7] The objects lack a great deal of physical strength until they are calcinated. In a medium with significant surface tension, they prefer to segregate themselves, causing a large change in their shape as the DMSO molecules are removed and are no longer able to support the overall structures.

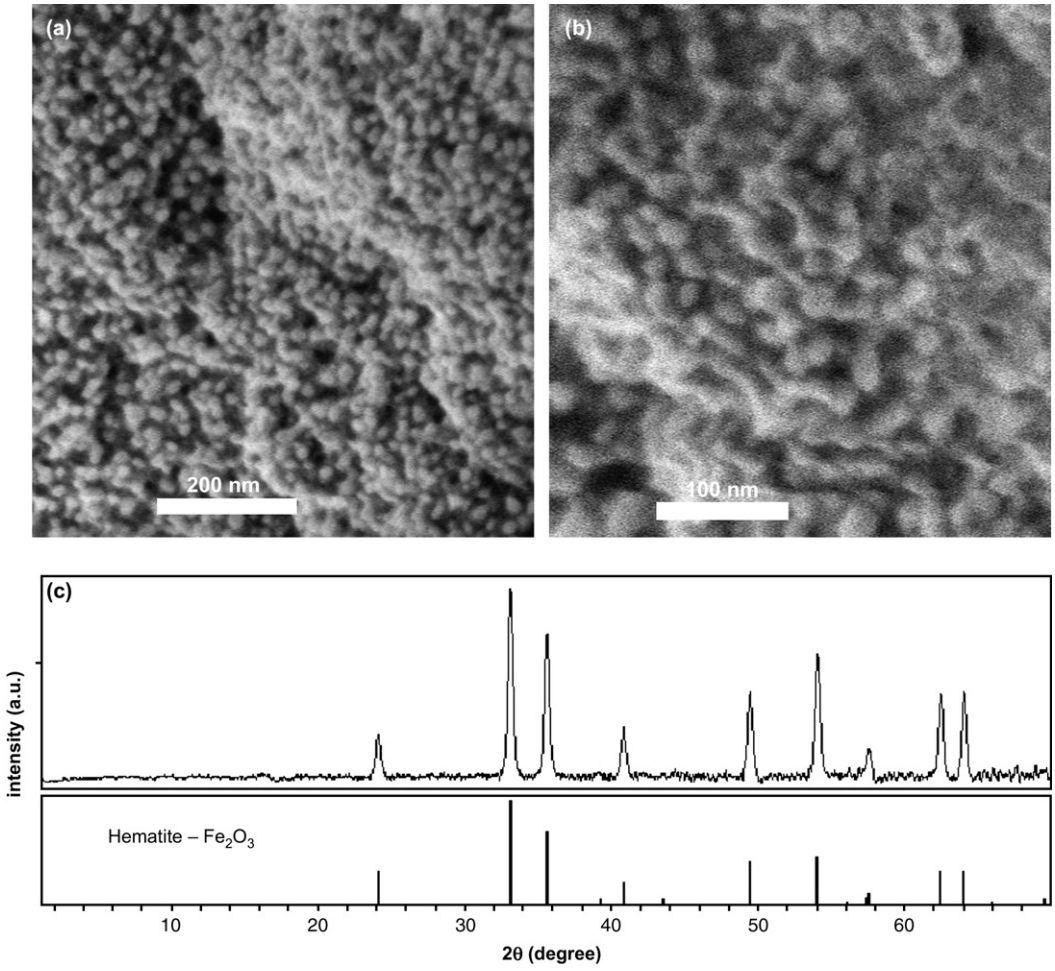

Figure 6. (a,b) SEM images of iron (III) oxide isolated from a gel comprised of 1 wt % HSA-S, $FeCl_3$/DMSO/H_2O (3:95:2, w/w/w) and aqueous ammonium hydroxide (see Section 4). The gel was aged for two weeks and calcinated. (c) Powder X-ray diffraction patterns of iron oxide obtained (top) and of α-Fe_2O_3 (hematite) from the Materials Data JADE (version 5.0.35) database.[23]

2.2.3. Templated iron oxide. Nanosized iron oxide particles, especially γ-Fe_2O_3 (maghemite), have been prepared in various systems,[28,20] such as in reverse micelles,[20a] organohydrogels,[28] and foams.[20b] The hydrolysis of ferric chloride (shown as Fe^{3+}) involves cationic intermediates (Eqs. 1–3).[21]

$$Fe^{3+} + H_2O \rightleftarrows Fe(OH)^{2+} + H^+ \quad (1)$$

$$Fe(OH)^{2+} + H_2O \rightleftarrows Fe(OH)_2^+ + H^+ \quad (2)$$

$$Fe(OH)_2^+ + H_2O \rightleftarrows Fe(OH)_3 + H^+ \quad (3)$$

When 10 molar equiv (with respect to Fe^{3+}) of 30% aqueous ammonium hydroxide were added to a 3 wt % $FeCl_3$ in DMSO solution (containing 2 wt % H_2O from the $FeCl_3 \cdot 6H_2O$ reagent) in the absence of HSA-S, a floc of brown precipitate was formed instead of a gel. This result does not eliminate the possibility that the gel formed in the presence of 1 wt % HSA-S is not based on Fe^{3+} as the cation for the HSA anions.

The cationic intermediates may have strong interactions with the anionic HSA-S molecular assemblies, such as the SAFINs in the organogels. In fact, Fe^{3+} and Na^+ ions may exchange at the fiber surfaces. If so, the shape of HSA-S molecular assemblies should be transferred to the iron oxide as in the silica cases, but by a very different mechanism.

'Necklace-like' iron oxide, consisting of particles with diameters of tens of nanometers (Fig. 6a and b), was obtained quantitatively (assuming that the product consists of Fe_2O_3 only). The powder X-ray diffraction patterns in Figure 6c demonstrate that the iron oxide obtained after calcinations is α-Fe_2O_3 (hematite), a well-known semiconductor.[22]

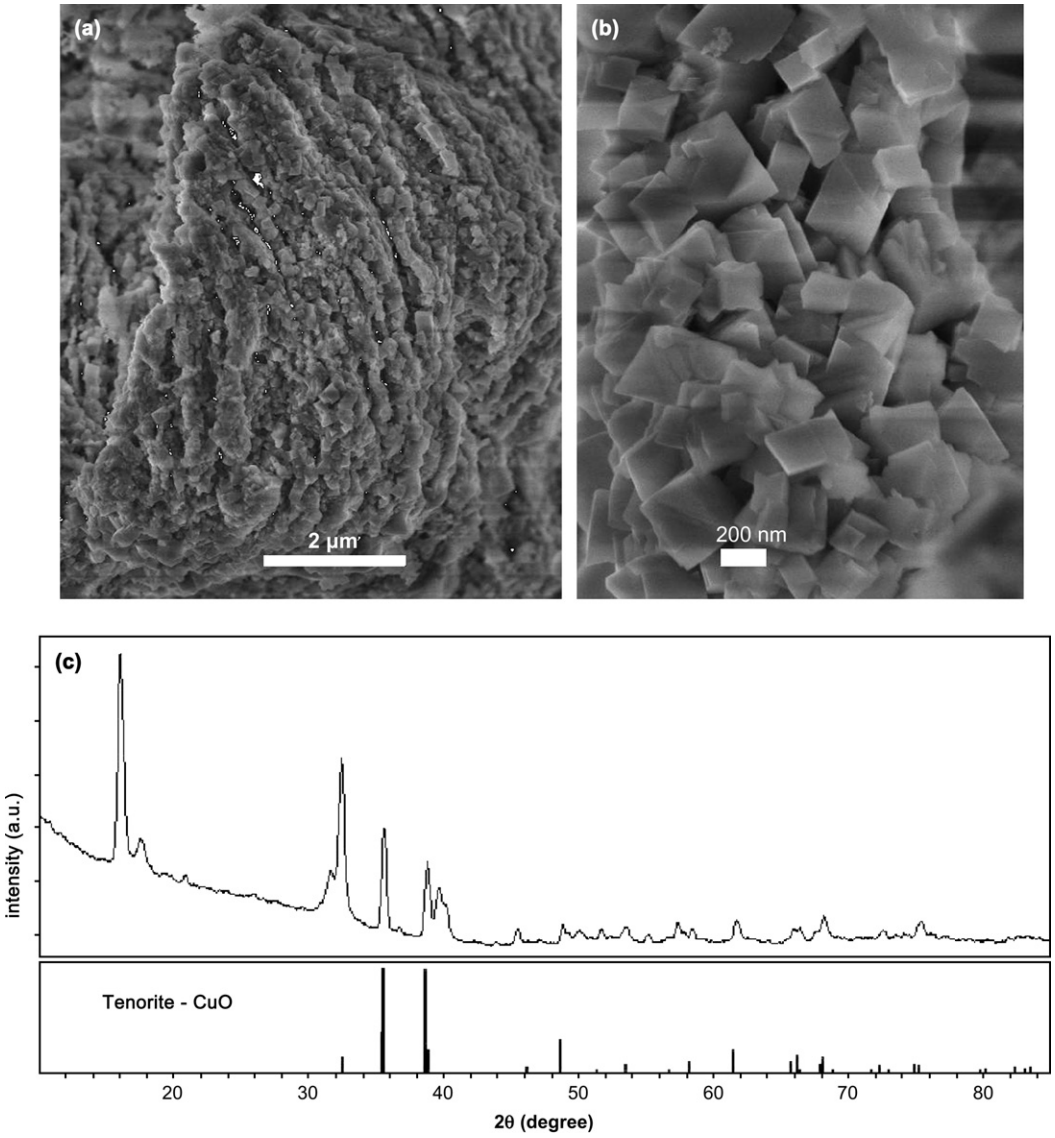

Figure 7. (a,b) SEM images of copper(II) oxide isolated from 1 wt % HSA-S and $CuCl_2/H_2O$ (7.9:91.1, w/w). (c) Powder X-ray diffraction patterns of copper oxide obtained (top) and of CuO (tenorite) from the Materials Data JADE (version 5.0.35) database.[23]

2.2.4. Templated copper(II) oxide. It was not possible to prepare a DMSO gel with HSA-S and $CuCl_2 \cdot 2H_2O$ because the copper salt did not dissolve. Thus, $CuCl_2 \cdot 2H_2O$ was added to an aqueous solution of HSA-S. The resulting suspension yielded nanosized copper(II) oxide crystals, which appear to be fiber-like arrays after drying and calcinations (Fig. 7a) but, at higher magnifications, they are shown to be somewhat organized aggregates of nanoparticles (Fig. 7b). The powder X-ray diffraction pattern in Figure 7c indicates that the material is a mixture of tenorite CuO (whose diffraction pattern is shown for comparison) and another morph or substance (not NaCl), which we have been unable to identify.

3. Conclusions

We have compared the efficiency of gelation of HSA-S with that of its parent acid, HSA, in a diverse selection of organic liquids. The sodium salt is a much better gelator, being able to form stable organogels with a wide variety of liquids, at even 0.5 wt %. The structures of the SAFINs from those gels consist of fibers in which the LMOGs are packed in bilayers.

Although these LMOGs are interesting because of their structures and efficiencies, and their gels are remarkable because of their thermal stabilities, their most important feature, perhaps, is their ability to promote the syntheses of templated nanoobjects of inorganic oxides. Thus, fiber-like silica objects with 'necklace' features have been made by sol–gel polymerizations of TEOS in several of the HSA-S and one of the HSA organogels. The driving force for templating in these cases is thought to be H-bonding or electrostatic interactions (using sodium ions as bridges) between the SAFIN surfaces and anionic silicate intermediates. These structurally simple and commercially available LMOGs eliminate one of the practical impediments to the widespread use of organogels to make templated nanomaterials. The accessibility of the LMOGs and their simple structures make them ideal candidates for future studies with other inorganic oxide precursors. Here, we have demonstrated that they can produce nanoparticles of iron and copper oxides using an analogous approach.

Simple variations of the protocols adopted here may result in even more robust and interesting inorganic oxide nanomaterials. Future experiments will be directed to optimize both the aspects of the templated materials.

4. Experimental section

4.1. Materials

Tetraethyl orthosilicate (TEOS, Aldrich, 99.9%), ammonium hydroxide (Fisher Scientific, 29.8%), glacial acetic acid (J. T. Baker, 99.9%), benzyl amine (Aldrich, 99%), NaOH (Fisher Scientific, GR), $FeCl_3 \cdot 6H_2O$ (J. T. Baker, certified reagent), and $CuCl_2 \cdot 2H_2O$ (J. T. Baker, certified reagent) were used as received. All solvents used are of GR grade or better and no attempt was made to dry them.

(*R*)-12-Hydroxystearic acid (HSA, Arizona chemicals, mp: 58.6–80.3 °C) was purified by three crystallizations from hot 95:5 hexane/ethyl acetate solutions under vigorous stirring (to avoid gelation):[24] mp 79.7–82.1 °C, $[\alpha]_D^{21}$ −0.49 (0.141 g/mL, in pyridine) (lit.[25] mp 79.3–79.8 °C, $[\alpha]_D^{19}$ −0.41 (0.168 g/mL, in pyridine)); elemental analysis: calcd for $C_{18}H_{36}O_3$, C 71.95, H 12.08, found C 72.22, H 12.14.

(*R*)-12-Hydroxystearic acid sodium salt (HSA-S) was synthesized by stirring 7.1 g of purified HSA and 1.1 g NaOH (molar ratio 1:1.1) in 300 mL of ethanol for 2–3 days. The solvent was removed on a rotary evaporator to yield a yellowish solid. After recrystallization from ethanol and ethyl acetate (gel formed in ethyl acetate, which was broken mechanically with a spatula), a white solid, mp 229.2–231.1 °C (lit.[26] mp 225 °C from differential scanning calorimetry), was obtained in 90% yield. Elemental analysis: calcd for $C_{18}H_{35}O_3Na$, C 67.05, H 10.94, found C 66.88, H 11.13.

4.2. Sample preparation and instrumentation

Melting points and optical micrograph (OM) images were recorded on a Leitz 585 SM-LUX-POL microscope equipped with crossed polars and a Photometrics CCD camera interfaced to a computer. The OM samples, flame-sealed in 0.4 mm pathlength, flatted, Pyrex capillary tubes (VitroCom), were heated to their liquid phase in a boiling water bath and then cooled in air (22 °C) until gelation occurred.

SEM and TEM images were recorded with 1–6 kV and 20 kV electron beam energies, respectively, on a Zeiss Supra 55 VP electron scanning microscope equipped with an add on STEM-D detector from Zeiss. Samples for scanning electron microscopy (SEM) were prepared by spreading powdered silica aliquots on conductive tape (M. E. Taylor Engineering, Inc.), which was attached to an Al mount (1/2″ slotted head, 1/8″ pin, Ted Pella, Inc.). No metal coating was applied. TEM samples were prepared by suspending silica in cyclohexane by sonicating for 5 min in a Bransonic 1210-R sonicator (Branson Ultrasonics Co.). A small drop of suspension was placed on a copper grid (200 mesh, Electron Microscopy Sciences Inc.) and the grid was dried under house-vacuum overnight.

X-ray diffraction (XRD) of samples sealed in 0.5 mm glass capillaries (W. Müller, Schönwalde, Germany) was performed on a Rigaku R-AXIS image plate system with Cu Kα X-rays (λ=1.54 Å) generated by a Rigaku generator operating at 46 kV and 46 mA with the collimator at 0.3 mm. Data processing and analyses were performed using Materials Data JADE (version 5.0.35) XRD pattern processing software.

4.2.1. Gelation test. Samples for gelation studies were prepared by placing known amounts of solvent and gelator in 5 mm (i.d.) glass tubes. The containers with the gel components were flame-sealed and then heated until the gelator completely dissolved. Thereafter, the hot solutions/sols were cooled in air (22 °C) until gelation occurred. Qualitatively, gelation was considered successful if no sample flow was observed upon inverting the container at room

temperature (i.e., the 'inverse flow' method[27]) after a third heating and cooling cycle. If part of the sample fell, the sample was classified as a partial gel.

Gelation temperatures were determined by inverting samples in sealed glass tubes and strapping them near the bulb of a thermometer, which can be read in 0.1 °C. The thermometer and sample were immersed in a stirred water bath at room temperature. It was warmed slowly. The range of temperatures in Table 1 reports when some of the gel sample fell initially and when the last part fell.

4.2.2. Hydrolytic sol–gel preparation. At least some water is essential in hydrolytic sol–gel process.[12] For that reason, the liquids used to make the gels for templating purposes were not dried; the liquids employed here contain sufficient amounts of water to initiate the sol–gel process.[7]

Weighed amounts of the HSA or HSA-S, solvent/TEOS (90:10, w/w), and catalyst were flame-sealed in a 5 mm (i.d.) glass tube. Detailed recipes for individual preparations are given in figure captions and in Section 2. The mixtures were heated in a boiling water bath until all solids dissolved, cooled in air to effect gelation of their sols (as confirmed by the inversion flow method[27]), and then left at room temperature for about one month (to allow the hydrolytic sol–gel process to proceed to completion). At the end of that period, one end of each tube was opened to atmosphere for 2–3 days at room temperature followed by another 2–3 days under a dynamic pressure of 460 Torr to dry the sample. Due to the high boiling point of DMSO, its gels were placed under 3 Torr for 4–5 days after the initial period in the atmosphere. The dried samples were calcinated by heating to 500 °C for a 4–6 h period and leaving them at that temperature for $\geq$2 h in a Fisher 182 Isotemp muffle furnace.

Percentage yields of silica after calcination were always >90% as calculated from the amounts of TEOS added and assuming that the silica obtained after calcinations consisted of $(SiO_2)_n$ only.

4.2.3. Iron oxide preparation. The procedure was adapted from Li et al.[28] Instead of starting with a gel,[28] our initial system, 1 wt % HSA-S and 3 wt % $FeCl_3$ in DMSO (containing 2 wt % H_2O), was a solution. However, when 30% aqueous ammonium hydroxide (a total of 10 molar equiv with respect to Fe^{3+}) was added dropwise, the solution gelled within a few minutes; a layer of excess ammonium hydroxide remained above the gel so that the precise water content in the gel is not known. The dark brown gel was aged for 2 weeks in the presence of the aqueous ammonium hydroxide layer, the aqueous layer was removed with a pipette, and the gel was dried and calcinated as described in the silica preparations.

4.2.4. Copper oxide preparation. HSA-S (2 wt %) in water was warmed until a clear sol was observed. At room temperature, 15.8 wt % aqueous $CuCl_2$ solution was added to the warm HSA-S sol; the final composition was 1 wt % HSA-S and 7.9 wt % $CuCl_2$ in water. Immediately, a green, thick suspension was obtained. Then, 10 molar equiv (with respect to Cu^{2+}) of 30 wt % aqueous ammonium hydroxide were added to assure 100% conversion to $Cu(OH)_2$. After a few hours, the sample was dried and calcinated as described above.

Acknowledgements

We thank the U.S. National Science Foundation for its support of this research and Mr. Paul Goldey and Professor Paola Barbara of the Department of Physics, Georgetown University for help in obtaining the SEM images.

References and notes

1. (a) Hu, J. T.; Odom, T. W.; Lieber, C. M. *Acc. Chem. Res.* **1999**, *32*, 435–445; (b) Burda, C.; Chen, X.; Narayanan, R.; El-Sayed, M. A. *Chem. Rev.* **2005**, *105*, 1025–1102; (c) Fernández-García, M.; Martínez-Arias, A.; Hanson, J. C.; Rodriguez, J. A. *Chem. Rev.* **2004**, *104*, 4063–4104.
2. (a) Lin, H.-P.; Mou, C.-Y. *Acc. Chem. Res.* **2002**, *35*, 927–935; (b) Wan, Y.; Yang, H.; Zhao, D. *Acc. Chem. Res.* **2006**, *39*, 423–432; (c) Huo, Q.; Margolese, D. I.; Clesta, U.; Feng, P.; Gler, T. E.; Sleger, P.; Leon, R.; Petroff, P. M.; Schuth, T.; Stucky, G. D. *Nature* **1994**, *368*, 317–321; (d) Lin, H. P.; Mou, C. Y. *Science* **1996**, *273*, 765–768; (e) Tanev, P. T.; Liang, Y.; Pinnavaia, T. J. *J. Am. Chem. Soc.* **1997**, *119*, 8616–8624; (f) Tolbert, S. H.; Firouzi, A.; Stucky, G. D.; Chmelka, B. F. *Science* **1997**, *278*, 264–268; (g) Kosuge, K.; Murakami, T.; Kikukawa, N.; Takemori, M. *Chem. Mater.* **2003**, *15*, 3184–3189; (h) Shimizu, T.; Masuda, M.; Minamikawa, H. *Chem. Rev.* **2005**, *105*, 1401–1444.
3. (a) Terech, P.; Weiss, R. G. *Chem. Rev.* **1997**, *97*, 3133–3159; (b) Abdallah, D. J.; Weiss, R. G. *Adv. Mater.* **2000**, *12*, 1237–1247; (c) *Molecular Gels: Materials with Self-Assembled Fibrillar Networks*; Weiss, R. G., Terech, P., Eds.; Springer: Dordrecht, 2006; (d) George, M.; Weiss, R. G. *Acc. Chem. Res.* **2006**, *39*, 489–497.
4. (a) Ono, Y.; Nakashima, K.; Sano, M.; Kanekiyo, Y.; Inoue, K.; Hojo, J.; Shinkai, S. *Chem. Commun.* **1998**, 1477–1478; (b) Jung, J. H.; Ono, Y.; Hanabusa, K.; Shinkai, S. *J. Am. Chem. Soc.* **2000**, *122*, 5008–5009; (c) Jung, J. H.; Kobayashi, H.; Masuda, M.; Shimizu, T.; Shinkai, S. *J. Am. Chem. Soc.* **2000**, *123*, 8785–8789; (d) Jung, H. J.; Ono, Y.; Shinkai, S. *Langmuir* **2000**, *16*, 1643–1649; (e) van Bommel, K. J. C.; Shinkai, S. *Langmuir* **2002**, *18*, 4544–4548; (f) Sugiyasu, K.; Tamaru, S.-i.; Takeuchi, M.; Berthier, D.; Huc, I.; Oda, R.; Shinkai, S. *Chem. Commun.* **2002**, 1212–1213; (g) Jung, J. H.; Shinkai, S. *J. Chem. Soc., Perkin Trans. 2* **2000**, 2393–2398.
5. (a) Clavier, G. M.; Pozzo, J. L.; Bouas-Laurent, H.; Liere, C.; Roux, C.; Sanchez, C. *J. Mater. Chem.* **2000**, *10*, 1725–1730; (b) Llusar, M.; Monrós, G.; Roux, C.; Pozzo, J. L.; Sanchez, C. *J. Mater. Chem.* **2003**, *13*, 442–444; (c) Llusar, M.; Roux, C.; Pozzo, J. L.; Sanchez, C. *J. Mater. Chem.* **2003**, *13*, 2505–2514.
6. (a) Moreau, J. J. E.; Vellutini, L.; Man, M. W. C.; Bied, C. *J. Am. Chem. Soc.* **2001**, *123*, 1509–1510; (b) Dautel, O. J.; Lère-Porte, J.-P.; Moreau, J. J. E.; Man, M. W. C. *Chem. Commun.* **2003**, 2662–2663.
7. Huang, X.; Weiss, R. G. *Langmuir* **2006**, *22*, 8542–8552.
8. Maskaev, A. K.; Man'kovskaya, N. K.; Lend'el, I. V.; Fedorovskii, V. T.; Simurova, E. I.; Terent'eva, V. N. *Chem. Technol. Fuels Oils* **1971**, *7*, 109–112.

9. (a) Terech, P.; Rodriguez, V.; Barnes, J. D.; Mckenna, G. B. *Langmuir* **1994**, *10*, 3406–3418; (b) Terech, P.; Pasquier, D.; Bordas, V.; Rossat, C. *Langmuir* **2000**, *16*, 4485–4494; (c) Tsau, J. S.; Heller, J. P.; Pratap, G. *Polym. Prepr.* **1994**, *35*, 737–738; (d) Tachibana, T.; Mori, T.; Hori, K. *Bull. Chem. Soc. Jpn.* **1980**, *53*, 1714–1719; (e) Tachibana, T.; Mori, T.; Hori, K. *Bull. Chem. Soc. Jpn.* **1981**, *54*, 73–80.
10. (a) McClellan, A. L. *J. Phys. Chem.* **1960**, *32*, 1271–1272; (b) Tachibana, T.; Kambara, H. *J. Colloid Interface Sci.* **1965**, *28*, 173–174; (c) Tachibana, T.; Kambara, H. *J. Am. Chem. Soc.* **1965**, *87*, 3015–3016; (d) Tachibana, T.; Kambara, H. *Bull. Chem. Soc. Jpn.* **1969**, *42*, 3422–3424.
11. We have been able to find only one report of HSA-S as an LMOG, and that to only with 1-alkanols: Tachibana, T.; Kitazawa, S.; Takeno, H. *Bull. Chem. Soc. Jpn.* **1970**, *43*, 2418–2421.
12. (a) Iler, R. K. *The Chemistry of Silica*; Wiley: New York, NY, 1979; pp 185, 213, 239; (b) Brinker, C. J.; Scherer, G. W. *Sol–Gel Science: The Physics and Chemistry of Sol–Gel Processing*; Academic: Boston, MA, 1990; pp 103–109; (c) Hench, L. L.; West, J. K. *Chem. Rev.* **1990**, *90*, 33–72.
13. Boner, C. J. *Manufacture and Application of Lubricating Greases*; Reinhold: New York, NY, 1960.
14. Luboradzki, R.; Gronwald, O.; Ikeda, A.; Shinkai, S. *Chem. Lett.* **2000**, *29*, 1148–1149.
15. Drits, V. A.; Tchoubar, C. *X-ray Diffraction by Disordered Lamellar Structures*; Springer: Berlin, 1990.
16. Estimated based on single crystal structure of racemic HSA: (a) Kuwahara, T.; Nagase, H.; Endo, T.; Ueda, H.; Nakagaki, M. *Chem. Lett.* **1996**, 435–436; (b) Kamijo, M.; Nagase, H.; Endo, T.; Ueda, H.; Nakagaki, M. *Anal. Sci.* **1999**, *15*, 1291–1292.
17. Badenhoop, J. K.; Weinhold, F. *J. Chem. Phys.* **1997**, *107*, 5422–5432.
18. (a) Spector, M. S.; Selinger, J. V.; Schnur, J. M. *Materials-Chirality*; Green, M. M., Nolte, R. J. M., Meijer, E. W., Eds.; Wiley: New York, NY, 2003; Chapter 5; (b) Aggeli, A.; Nyrkova, I. A.; Bell, M.; Harding, R.; Carrick, L.; McLeish, T. C. B.; Semenov, A. N.; Boden, N. *Proc. Natl. Acad. Sci. U.S.A.* **2001**, *98*, 11857–11862.
19. Surface tensions are 28.88 mN/m for benzene at 20 °C, 22.39 mN/m for ethanol at 20 °C, 43.54 mN/m for DMSO at 20 °C, and 26.50 mN/m for THF at 25 °C.[19a] (a) *Dean's Handbook of Organic Chemistry*, 2nd ed.; Gokel, G. W., Ed.; McGraw-Hill: New York, NY, 2004; pp 4–55.
20. (a) Pillai, V.; Kumar, P.; Hou, M. J.; Ayyub, P.; Shah, D. O. *Adv. Colloid Interface Sci.* **1995**, *55*, 241–269; (b) Shankar, S. S.; Patil, U. S.; Prasad, B. L. V.; Sastry, M. *Langmuir* **2004**, *20*, 8853–8857.
21. (a) Gregory, J.; Duan, J. *Pure Appl. Chem.* **2001**, *73*, 2017–2026; (b) Cornell, R. M.; Schwertmann, U. *The Iron Oxides: Structure, Properties, Reactions, Occurrence and Uses*, 2nd ed.; VCH: Weinheim, 2003.
22. Cotton, F. A.; Wilkinson, G. *Advanced Inorganic Chemistry*, 5th ed.; Wiley: New York, NY, 1988; pp 711–712.
23. Diffraction pattern was matched by the database of the software package: Materials Data JADE (version 5.0.35).
24. George, M.; Weiss, R. G. Unpublished results.
25. Serck-Hanssen, K. *Chem. Ind.* **1958**, 1554.
26. Abrams, S. T.; Stross, F. H. *J. Phys. Chem.* **1958**, *62*, 879–880.
27. Eldridge, J. E.; Ferry, J. D. *J. Phys. Chem.* **1954**, *58*, 992–995.
28. Li, S.; John, V. T.; Rachakonda, S. H.; Irvin, G. C.; McPherson, G. L.; O'Connor, C. J. *J. Appl. Phys.* **1999**, *85*, 5178–5180.